Pursuit Law Development and Implementation for the Interception of Hypersonic Vehicles

Gavin Armstrong, Gabriel Colangelo
University at Buffalo, Department of Mechanical and Aerospace Engineering

***Abstract* – This paper will discuss various pursuit laws which can be utilized to intercept a vehicle traveling at hypersonic speeds. For clarification, hypersonic speed refers to speeds greater than Mach 5. The various pursuit laws discussed in this paper are pure pursuit, proportional navigation (more specifically ideal proportional navigation), and motion camouflage. Each pursuit law will be briefly derived, and a simple example of implementation will be shown, using a MATLAB simulation.**

***Keywords* – Motion Camouflage, Proportional Navigation, Pure Pursuit**

NOMENCLATURE

r	Distance between target and pursuer.
θ	Line of Sight (LOS) angle
λ	Proportional Navigation Constant.

I. INTRODUCTION

This paper will discuss the development of pursuit/guidance laws which can be used in the interception of hypersonic vehicles. The three specific pursuit laws discussed are proportional navigation, pure pursuit, and motion camouflage. For the implementation of these pursuit laws, the following modeling assumptions are made: The model assumes a two-dimensional, planar system with a pursuer and a target, both represented by point masses of similar mass properties. This assumption allows us to make the statement that both masses have the same mass, moment of inertia, and aerodynamic coefficients. Because of this, we can neglect the effects of certain external forces such as drag and gravity.

A figure representing the general layout of our model is given below.

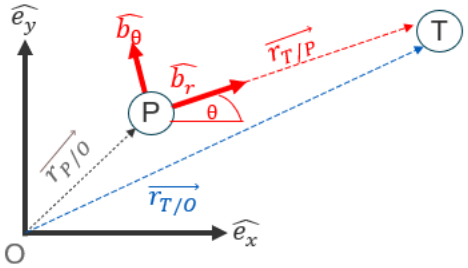

Fig. 1. Kinematic Model

In Figure 1, the pursuer vehicle is represented by mass P, and the target vehicle is represented by mass T. There are two reference frames, an inertial frame, I, represented by $(\hat{e}_x,\hat{e}_y,\hat{e}_z)$, with origin O and the line of sight frame, B, with an origin at mass P. The B frame has the unit vector $\hat{b}_r$ aligned with the line of sight from P to T, and the $\hat{b}_\theta$ unit vector is the direction vertical to $\hat{b}_r$. The last unit vector $\hat{b}_z$ is the cross product of $\hat{b}_r$ and $\hat{b}_\theta$. The relative distance between the target and the pursuer along the line of sight is given by $\vec{r}_{T/P}$. The angle between the line of sight and the inertial $\hat{e}_x$ is given by θ. The relative distance, $\vec{r}_{T/P}$ can be expressed using polar coordinates as:

$$\vec{r}_{T/P} = \vec{r}_{T/O} - \vec{r}_{P/O} = r\hat{b}_r \tag{1}$$

The relative velocity between the target and interceptor can be found by applying the transport theorem on the relative position vector $\vec{r}_{T/P}$. Using polar coordinates, the relative velocity vector expressed in the B frame (LOS frame) can be obtained as:

$$\vec{v}_{T/P} = \dot{r}\hat{b}_r + r\dot{\theta}\hat{b}_\theta \tag{2}$$

Then the transport theorem can be applied once more on the relative velocity vector, generating the relative acceleration vector as observed in the B frame. This yields:

$$\vec{a}_{T/P} = (\ddot{r} - r\dot{\theta}^2)\hat{b}_r + (2\dot{r}\dot{\theta} + r\ddot{\theta})\hat{b}_\theta \tag{3}$$

Furthermore, Newton's 2nd law can be applied on the two point masses. The net forces on the target and pursuer are represented by F_T and F_P respectively. Dividing F_T and F_P by their mass, m, results in the acceleration caused by external/applied forces, which we will call u_T and u_P. The relative acceleration can also then be expressed as:

$$\vec{a}_{T/P} = \vec{a}_{T/O} - \vec{a}_{P/O} = \frac{F_T}{m} - \frac{F_P}{m} = u_T - u_P \tag{4}$$

Equation 3 can be broken up into 2 second order ordinary differential equations. Later in this paper, the results of the pursuit law implementations will be displayed. These simulations were run using MATLAB's 4th order Runge-Kutta integrator, ODE45, on a state space model. The states used in this model are defined below.

$$\vec{x} = \begin{pmatrix} x_1 \\ x_2 \\ x_3 \\ x_4 \end{pmatrix} = \begin{pmatrix} r \\ \dot{r} \\ \theta \\ \dot{\theta} \end{pmatrix} \tag{5}$$

II. Proportional Navigation

The first type of pursuit law discussed will be proportional navigation. There are multiple forms of proportional navigation, such as Generalized Proportional Navigation, Pure Proportional Navigation, and True Proportional Navigation (Kibo, Taotao, and Lei). This paper will specifically focus on Ideal Proportional Navigation (IPN). For Ideal Proportional Navigation, the commanded acceleration is applied in the direction normal to the relative velocity between the interceptor and its target, and its magnitude is proportional to the product of LOS rate and relative velocity (Yuan and Chern). For 2D IPN with a non-maneuvering target, the command acceleration can be calculated using the following equation, where λ is the Proportional Navigation Constant and $\dot{\theta}$ is the LOS angular rate (Yuan and Chern):

$$\vec{a}_c = \lambda \dot{\theta} \hat{b}_z \times \vec{v}_{T/P} = \lambda(-r\dot{\theta}^2 \hat{b}_r + \dot{r}\dot{\theta}\hat{b}_\theta) \tag{6}$$

For a non-maneuvering target, u_T is zero, therefore by letting $-u_P$ be equal to $\vec{a}_c$, the substitution of equation 6 into equation 3 can be made such that:

$$(\ddot{r} - r\dot{\theta}^2)\hat{b}_r + (2\dot{r}\dot{\theta} + r\ddot{\theta})\hat{b}_\theta = \lambda(-r\dot{\theta}^2\hat{b}_r + \dot{r}\dot{\theta}\hat{b}_\theta) \tag{7}$$

Equation 7 is actually two coupled second order ordinary differential equations, which are shown below.

$$\ddot{r} - r\dot{\theta}^2 = -r\lambda\dot{\theta}^2 \tag{8}$$

$$2\dot{r}\dot{\theta} + r\ddot{\theta} = \lambda\dot{r}\dot{\theta} \tag{9}$$

It is shown in Yuan and Chern that in the case of IPN for both a maneuvering and non-maneuvering target, the capture condition is simply $\lambda > 1$. The only exception is for the initial conditions $\dot{r} > 0$ and $\dot{\theta} = 0$ (Kibo, Taotao, and Lei). λ is typically chosen to be a value between 3 and 6 as both the command acceleration and LOS angular rate will approach infinity if $\lambda \leq 2$ (Yuan and Chen). It is also worth noting a few characteristics of IPN that occur during the interception period for a non maneuvering target. If $\lambda > 2$, the LOS angular rate, $\dot{\theta}$, will approach zero meaning that the LOS angle will become constant during the interception period (Yuan and Chern). It can also be shown that the magnitude of the relative velocity is maintained at a constant, during the intercept period (Yuan and Chern). Both of these phenomena can be observed in the simulation results shown further on in the paper.

A closed form solution for the relative velocity is derived in Kibo, Taotao, and Lei. This solution is shown below, where $\dot{r}_0$ is the initial closing velocity and r_0 is the initial range-to-go/relative distance.

$$\dot{r} = \dot{r}_0^2 + r_0^2\dot{\theta}_0^2[1 - (\frac{r}{r_0})^{2(\lambda-1)}] \tag{10}$$

It should also be noted that there exists a closed form solution for the total interception time for IPN of a non-maneuvering target, which is derived in both Yuan and Chern and in Kibo, Taotao, and Lei. As such, we refer the reader to these papers for further information on this closed form solution.

For practical interception, pursuer acceleration capability is non-infinite. Therefore, it is worth going through the calculation of the command acceleration magnitude. The command acceleration is a vector quantity whose magnitude can be calculated using the Euclidean norm. Therefore, the magnitude of the command acceleration is given by (Kibo, Taotao, and Lei):

$$||\vec{a}_c|| = \lambda\sqrt{(r\dot{\theta}^2)^2 + (\dot{r}\dot{\theta})^2} \tag{11}$$

Equations 8 and 9 can be broken into 4 first order ordinary differential equations by putting them into state space form. Using the states defined in Equation 5, the following state space model is derived.

$$\dot{\vec{x}} = \begin{pmatrix} x_2 \\ (1-\lambda)x_1x_4^2 \\ x_4 \\ (\lambda-2)\frac{x_2x_4}{x_1} \end{pmatrix} \tag{12}$$

Using the state space model above, an IPN pursuit law can be implemented and simulated using MATLAB. The interception scenario has the following initial conditions: An initial range to go, r_0, of 150 km, and initial closing velocity of 1500 m/s, an initial LOS angular rate of 1 deg/s, with an initial LOS angle of 10 deg. If the simulation is assumed to occur at an altitude of 15 km, the speed of sound at this altitude is roughly 295 m/s. Using the initial conditions and taking the magnitude of equation 2, it can be calculated that the target is initially moving away from the pursuer at Mach 10. Therefore, IPN is being utilized for the interception of a hypersonic vehicle. The figures below show the trajectory using with an IPN pursuit law, and the trajectory with no guidance.

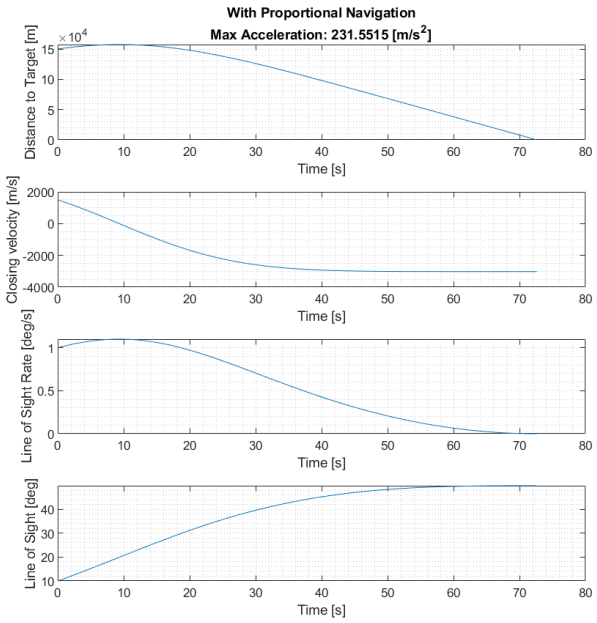

Fig. 2. Implementation of 2D IPN with a Non-Maneuvering Target

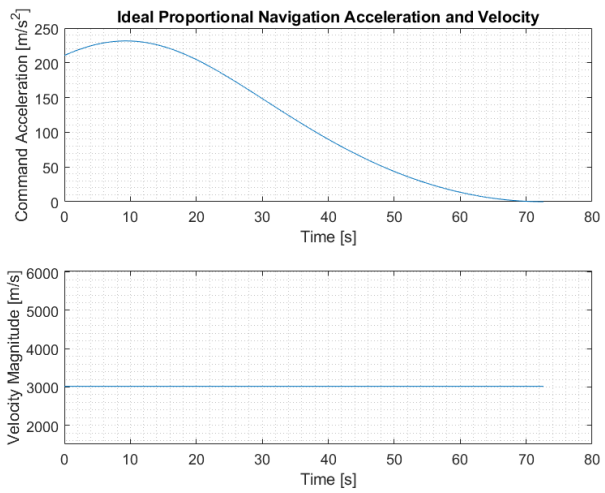

Fig. 3. Implementation of 2D IPN with a Non-Maneuvering Target - Acceleration Command and Relative Velocity Magnitude

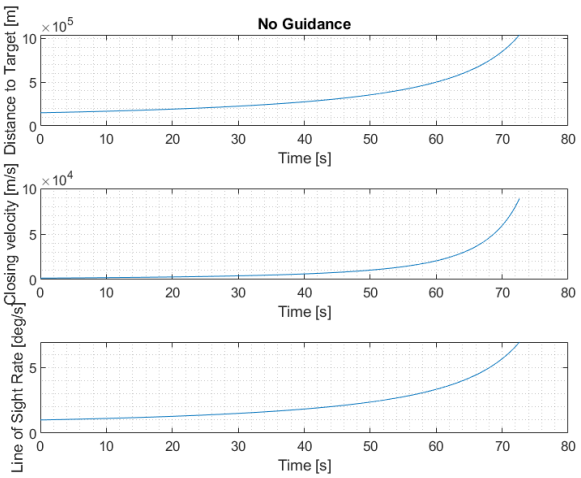

Fig. 4. Simulation With No Guidance

Looking at the results in Figure 2, it is seen that the interception time is 72 seconds. At this point the range to go distance goes to 0, signifying interception. During the interception period, it is also observed that the LOS angular rate approaches zero, while the relative velocity maintains a constant magnitude as shown in Figure 3. Both of these are observations are expected per Yuan and Chern. For interception, the maximum command acceleration needed was 231.5 $\frac{m}{s^2}$ or 23.5g (see Figure 3). Further on, a minor investigation on the effect of the navigation constant on the maximum command acceleration will be introduced. From Figure 4, it is shown that without the implementation of a pursuit law, the target moves infinitely far from the pursuer and no interception occurs.

A series of simulations were ran using the same initial conditions, but λ was varied from values ranging from 3 to 7. The maximum acceleration and time for interception are tabulated below.

TABLE I
Navigation Constant Analysis

λ	$t_{intercept}$ [s]	Max Acceleration $\frac{m}{s^2}$
3	84.18	173.66
4	72.62	231.55
5	66.88	289.44
6	63.44	347.33
7	61.15	405.22

From the table, it can be seen that the change in intercept time from λ equals 5 to 6, or 6 to 7 is only a few seconds, but the maximum acceleration increases 50 $\frac{m}{s^2}$. From this it can be concluded that there is not much benefit in increasing the navigation constant past 5. The most acceleration efficient jump in λ is when it is increased from 3 to 4, where we see a 12 second decrease in intercept time, at the cost of 58 $\frac{m}{s^2}$. For these initial conditions, $\lambda = 4$ is the optimal value. The value of λ is important, and it has a direct effect on the maximum acceleration command. For example, if the pursuer is only capable of a maximum acceleration of 200 $\frac{m}{s^2}$, $\lambda > 3$ is not a feasible control gain for these given initial conditions.

It is now worth introducing IPN for a maneuvering target ($u_T \neq 0$). It is assumed that the target will maneuver normal to the relative velocity, in order to resist the relative velocity turning to the direction of the LOS (Yuan and Chern). The equations of motion for IPN of a maneuvering target are given below (Yuan and Chern), where v is the magnitude of the relative velocity vector (Kibo, Taotao, and Lei).

$$v = \sqrt{\dot{r}^2 + r^2\dot{\theta}^2} \tag{13}$$

$$\ddot{r} - r\dot{\theta}^2 = -r\lambda\dot{\theta}^2 + \frac{u_T}{v}r\dot{\theta} \tag{14}$$

$$2\dot{r}\dot{\theta} + r\ddot{\theta} = \lambda\dot{r}\dot{\theta} - \frac{u_T}{v}\dot{r} \tag{15}$$

These equations can be put into state space form and simulated similarly to the way it was done in the non-maneuvering case. Equations 14 and 15 are highly non-linear and a closed form solution is difficult to obtain (Kibo, Taotao, and Lei). However, certain observations can be made. Like the non-maneuvering case, the capture criteria is still $\lambda > 1$ and magnitude of v is constant during the interception period. The relative velocity is constant during the intercept period because both the commanded acceleration and the target maneuver are applied in the same direction, normal to the relative velocity. Unlike the non-maneuvering target case, the LOS angular rate, $\dot{\theta}$ will never approach zero due to the target maneuvers (Yuan and Chern).

Lastly, the feedback law used for pure proportional navigation (PPN) will be introduced as it is referenced later in the motion camouflage discussion. For PPN, the command acceleration is applied in the direction normal to the interceptor velocity (Yuan and Chern). For the case of planar pursuit case, the pursuit law used for PPN is given by the following equation, where λ is the dimensionless navigation constant, and $\dot{\theta}$ is the

rate of rotation of the LOS vector (Justh and Krishnaprasad).

$$u^{PPN} = \lambda \dot{\theta} \tag{16}$$

The next pursuit law discussed is the case of simple, or pure, pursuit.

III. Pure Pursuit

A. Kinematic Analysis and Derivation

Pure pursuit, sometimes referred to as simple pursuit, is a pursuit law that in its purest form has the pursuer try to align its velocity vector (or a line along a physical body axis on the pursuer) with the current position of the target at the current time. Geometrically this can be seen as the overlaying of the velocity vector or body axis line directly along the target LOS (Shneydor). Pure pursuit is one of the earliest pursuit algorithms to be applied to the case of missile guidance, with its earliest applications being in the mid 20th century, and while it does have the virtue of simplicity its performance is generally lesser than more modern pursuit laws such as proportional navigation. A major reason for this is that for the pursuit of a moving target pure pursuit will lead to a tail chase where the pursuer must be faster than the target and close the range in the same direction of travel, placing great and possibly untenable requirements on total energy available to the pursuer. Additionally, the requirement of pointing towards the target directly can result in demands placed on the pursuer that are greater than those that can be supplied by the vehicle's capacity to turn or accelerate. This is especially true if the initial angle between the pursuer and LOS is significant.

Pure pursuit can be divided into two predominant categories: velocity pursuit and attitude pursuit. Velocity pursuit requires the overlaying of the velocity vector of the pursuer directly on the LOS to the target whereas attitude pursuit calls for a body axis vector of the pursuer to be directed towards the target. This can, for example, be the longitudinal body axis of an aircraft and can be useful in application due to the nature of sensors for detecting the LOS to the target being mounted on the body. Between the two methods, velocity pursuit provides more accurate guidance (Shneydor) but may not be applicable in all cases. This paper will examine 2D planar velocity pursuit, attitude pursuit is quite similar in implementation but given the greater accuracy velocity pursuit was chosen for analysis. To better represent the case of planar pure pursuit under investigation in this paper, the general kinematics of a pursuer and non-maneuvering target in a 2D plane can be examined as is shown below.

A generalized diagram of the geometry of planar pure pursuit can be seen in the next figure, with significant angles labeled where appropriate:

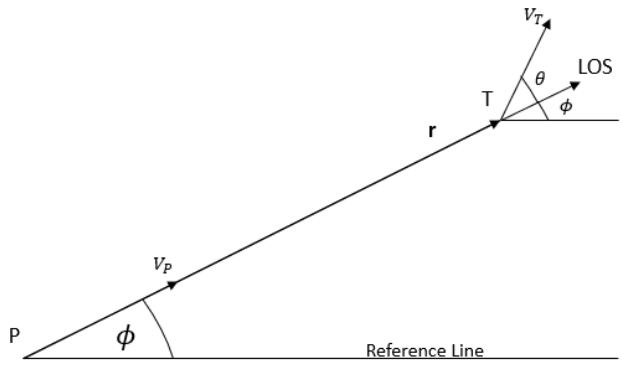

Fig. 5. Geometry of Pure Planar Pursuit

The angle ϕ represents the angle made by the LOS relative to some horizontal reference (taken to be inertial), the angle θ is the angle made between the velocity vector of the target and the LOS, P and T represent the pursuer and target, respectively, with their associated velocities V_P and V_T. r is the range between the two objects and the reduction of r to zero is the primary goal of the pursuit. A composite angle γ for both the target and pursuer as the total angle made of their velocity vectors with respect to the reference line. In the case of the target this would be $\gamma_T = \phi + \theta$.

For the kinematic derivations below and subsequent guidance implementation it is assumed that both the pursuer and target travel at constant velocities and do not accelerate tangentially during the course of the pursuit and intercept. The kinematics of the pursuer relative to the target are of more interest for pure pursuit than the target and pursuer's inertial kinematics, in terms of r, θ, and ϕ. It can be seen that the relative velocity of the target with respect to the pursuer for pure pursuit is:

$$\vec{v}_{T/P} = \vec{V}_T - \vec{V}_P \tag{17}$$

The velocity for the pursuer and target can be found using the geometry in Figure 5 and the Line of Sight frame described in the introduction as:

$$\vec{V}_T = V_T \, cos\theta \, \hat{b}_r - V_T \, sin\theta \, \hat{b}_\theta \tag{18}$$

Since in the case of pure pursuit the velocity vector of the pursuer lies along the LOS to the target, the velocity of the pursuer is simply:

$$\vec{V}_P = V_P \, \hat{b}_r \tag{19}$$

Substituting Equation 18 and Equation 19 into Equation 17 and equating the result to Equation 2 yields the kinematics for planar pure pursuit:

$$\dot{r} = V_T \, cos\theta - V_P \tag{20}$$

$$r\dot{\theta} = -V_T \, sin\theta \tag{21}$$

Equation 21 can be directly represented in first order form by dividing through by r which yields:

$$\dot{\theta} = -\frac{V_T}{r} sin\theta \tag{22}$$

Equations 20 and 22 can then be numerically integrated with the following state space model due to the equations being first order:

$$\vec{x} = \begin{pmatrix} x_1 \\ x_2 \end{pmatrix} = \begin{pmatrix} r \\ \theta \end{pmatrix}$$

A simulation was performed to demonstrate the ideal behavior for planar pure pursuit with an initial range of 100,000 meters, an initial θ of 90 degrees, V_T = 6,000 m/s, and V_P = 7,000 m/s. A break condition was set for when r fell below 0.001 meters, and plots of the resulting range and θ can be seen below:

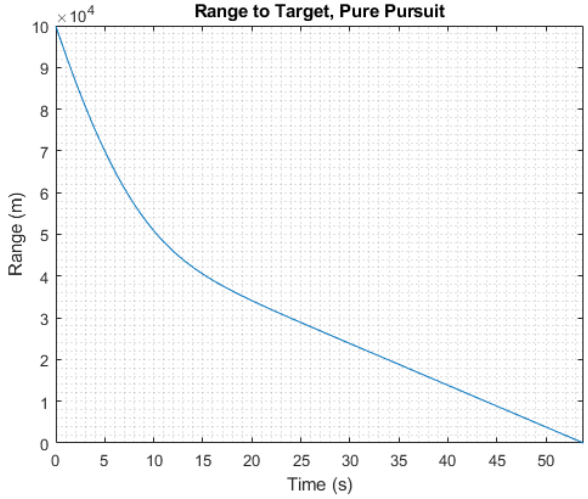

Fig. 6. Range to Target, Pure Pursuit

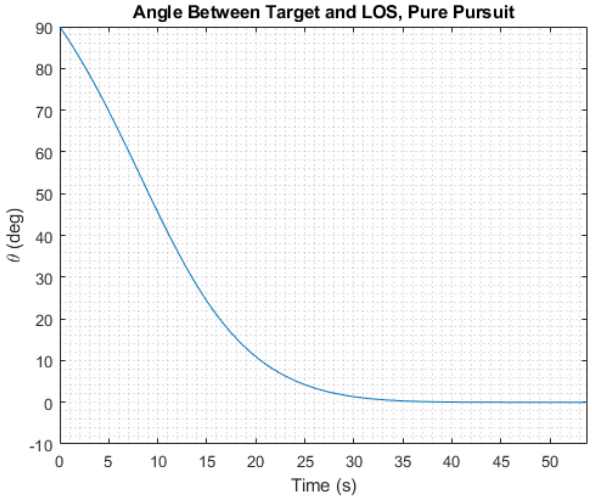

Fig. 7. Angle Between Target and LOS, Pure Pursuit

Examining Figure 6 the curvature of the range over time line can be seen to start parabolic and remain so until approximately 25 seconds where the angle between V_T and the LOS begins to become very small as seen in Figure 7 where it then becomes linear for the remainder of the simulation. This change of curvature corresponds to when the pursuit becomes a tail chase and the pursuer is directly behind the target. As such for pure pursuit the pursuer must be faster than the target for a successful interception, otherwise the target will remain at a set distance from the pursuer or increase the range for the cases of $V_T = V_P$ and $V_T > V_P$, respectively. Plots of the range for those two cases can be seen below, in the case for equal velocity V_T and V_P are both set to 6000 m/s and where $V_T > V_P$ their velocities are 6000 m/s and 5000 m/s, respectively. All other parameters are the same as those for the simulation demonstrated in Figures 6 and 7.

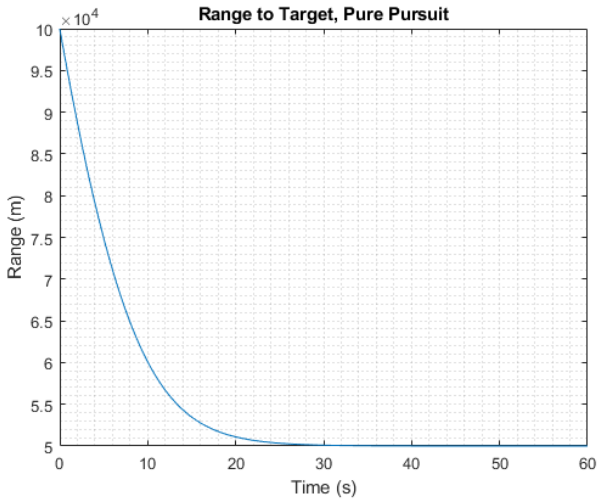

Fig. 8. Range to Target, Pure Pursuit, $V_T = V_P$

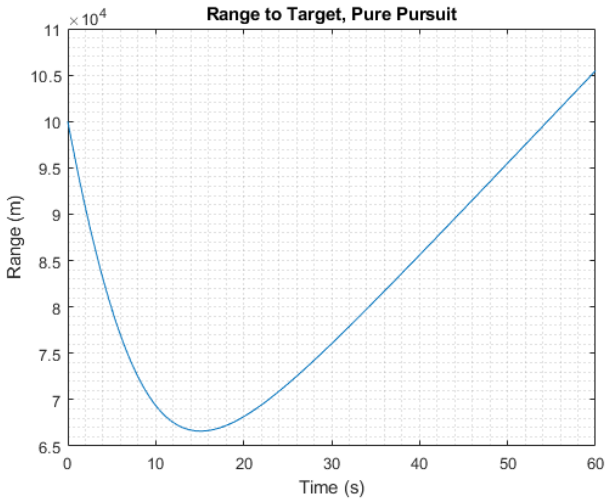

Fig. 9. Range to Target, Pure Pursuit, $V_T > V_P$

Figure 8 shows the parabolic decrease in range seen in Figure 6 but instead of changing to a linear decrease in range as the pursuer overhauls the target in a tail chase, the range settles at a nonzero value for the rest of the simulation run time. The range decreases during the initial turn as to align the LOS with the velocity vector of the target the pursuer must turn inside the target, giving a shorter path. Similar behavior is seen in Figure 9 where the range to the target again begins parabolic but changes in sign around 15 seconds and increases before then becoming linear as a tail chase is achieved with the target gaining distance on the pursuer until a range greater than the initial 100,000 meters is reached by the end of the simulation time. Approaches like deviated pursuit are modifications of the pure pursuit law which seek to address the shortcomings of pure pursuit such as lead pursuit where instead of laying the velocity vector directly on the target LOS the velocity vector is instead aligned ahead of the target LOS by some angle which creates a shorter path to the target. This approach, while not directly addressed in this paper, motivates the derivation of the guidance law which will seek to accomplish pure pursuit as shown in the following section.

B. Guidance Law Derivation and Implementation

The goal of the guidance law for pure pursuit is to create the scenario where the velocity vector of the pursuer is directly aligned with the target LOS from some deviated position. This deviation from the desired direction of travel can be represented with an angle δ, as shown in the following diagram.

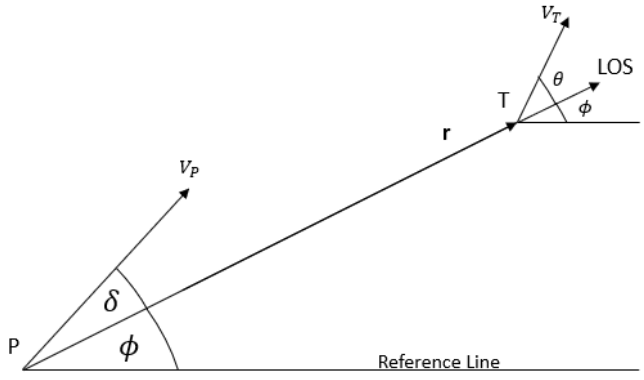

Fig. 10. Geometry of Pure Pursuit Guidance

As discussed for the target in the previous section an angle γ_P can be defined as $\gamma_P = \phi + \delta$ which represents the angle between the velocity vector of the pursuer and the reference line. The guidance law then should seek to drive δ to zero over time, satisfying the requirements of velocity pure pursuit. This can be accomplished by redefining δ in terms of γ_P and ϕ via the following relation:

$$\delta = \gamma_P - \phi \tag{23}$$

In order to implement and simulate a guidance law to accomplish pure pursuit, the kinematics for the scenario where V_P is not strictly on the LOS must be found. These are very similar to those found in the previous section, with the exception that $\vec{V_P}$ is now given by:

$$\vec{V_P} = V_P \cos\delta\, \hat{b}_r + V_P \sin\delta\, \hat{b}_\theta \tag{24}$$

Combining this with the previously found expressions in Equations 17 and 18 and equating the result with Equation 2 results in the following:

$$\dot{r} = V_T \cos\theta - V_P \cos\delta \tag{25}$$

$$r\dot{\theta} = V_P \sin\delta - V_T \sin\theta \tag{26}$$

As before, Equation 26 is divided through by r to yield a first order form for $\dot{\theta}$:

$$\dot{\theta} = \frac{V_P}{r} \sin\delta - \frac{V_T}{r} \sin\theta \tag{27}$$

Since the target is assumed to not maneuver ($\dot{\gamma_T} = \dot{\phi} + \dot{\theta} = 0$), Equation 27 can be used to yield an expression for the rate of change of the LOS angle ϕ:

$$\dot{\phi} = \frac{V_T}{r} \sin\theta - \frac{V_P}{r} \sin\delta \tag{28}$$

The guidance law $\dot{\gamma_P}$ is set to be the following (Shneydor):

$$\dot{\gamma_P} = \frac{-k V_P}{r} \sin\delta \tag{29}$$

Where k is some proportionate constant.

In order to implement and simulate the guidance law the state space model from the previous section was modified to include γ_P and ϕ like so:

$$\vec{x} = \begin{pmatrix} x_1 \\ x_2 \\ x_3 \\ x_4 \end{pmatrix} = \begin{pmatrix} r \\ \phi \\ \gamma_P \\ \theta \end{pmatrix}$$

One quantity of note is the lateral acceleration required of the pursuer to drive δ to zero, a centripetal quantity. This can be simply found via the following relation (Shneydor):

$$a_P = V_P \dot{\gamma_P} \tag{30}$$

Equations 29 and 30 show that the required lateral acceleration is proportionate to the velocity of the pursuer as well as the range, with lower ranges resulting in higher demanded lateral accelerations. This is intuitive, as aligning the velocity vector with the LOS over a shorter distance requires a tighter turn to be made. Additionally, to guarantee that $a_P \to 0$ as $r \to 0$ the constant k in Equation 29 must be greater than 2 (Shneydor).

The kinematics and guidance law given by Equations 25, 27, 28, and 29 were then implemented into a MATLAB simulation with similar conditions to those used for the kinematic analysis of pure pursuit in the previous section. The initial range was again taken to be 100,000 meters, V_P was taken to be 7,000 m/s, V_T 6,000m/s, ϕ $\frac{\pi}{6}$ rad, γ_P $\frac{\pi}{2}$ rad, and θ $\frac{\pi}{3}$ rad. The constant k was set to 3 for all simulation runs with this guidance law. The simulation was set to run until an intercept was successful with the same condition as

the previous section or to a maximum of 90 seconds. The results for the range to the target over time can be seen in the following figure:

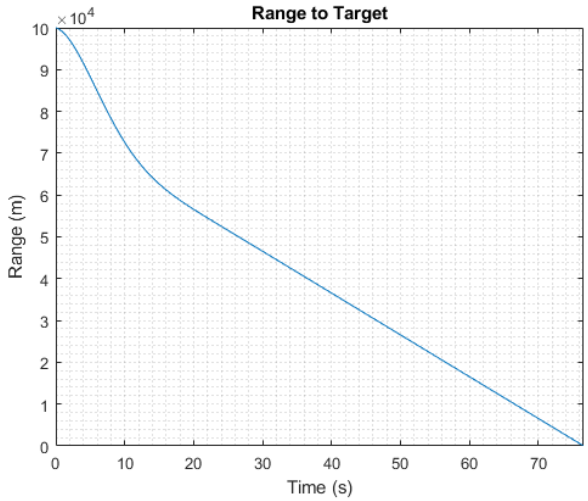

Fig. 11. Range to Target, Pure Pursuit Guidance

It can be seen that the range decreases initially in a nonlinear fashion, appearing to possibly be sinusoidal or greater than second order up until approximately 20 seconds at which point a tail chase is achieved and the pursuer overhauls the target until an interception at approximately 76 seconds. Plots of the LOS angle ϕ and the angle γ_P (in degrees) were also generated and collected into the figure below:

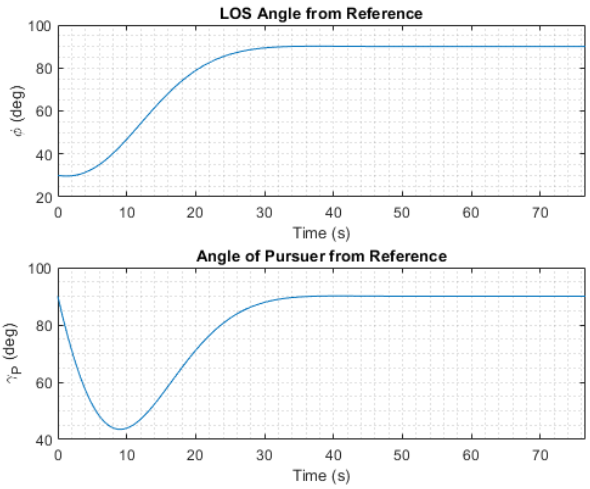

Fig. 12. ϕ and γ_P, Pure Pursuit Guidance

This demonstrates that despite starting at differing angles from the reference giving an initial δ of 60 degrees, the guidance law did successfully align the pursuer velocity vector with the target LOS. This shows that the deviation δ was decreased to zero by approximately 30 seconds, which corresponds to the linear behavior seen in Figure 11 at approximately the same time, satisfying pure pursuit. The angle between the velocity vector of the target and the LOS over the simulation run time, θ, was also captured in the following plot:

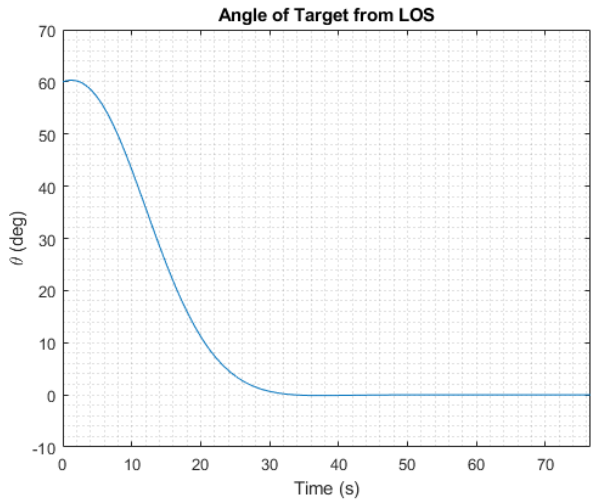

Fig. 13. Angle Between $\vec{V_T}$ and LOS, Pure Pursuit Guidance

As expected with the alignment of the pursuer velocity vector and the target LOS, the angle between the target's velocity vector and the LOS was driven to zero by approximately 30 seconds. This results in the tail chase which can be seen in the behavior of the previous two plots by the 30 second mark with the pursuer then gaining on the target until interception.

This successful interception did however take a great deal of time for the range being covered, taking about the same amount of time as the proportional navigation case but for a distance only 2/3 that used for that simulation. Additionally, the required lateral acceleration of the pursuer to achieve the pure pursuit case was very large, especially when compared to that achieved in the IPN case. A plot of the lateral acceleration over the run time of the simulation can be seen below:

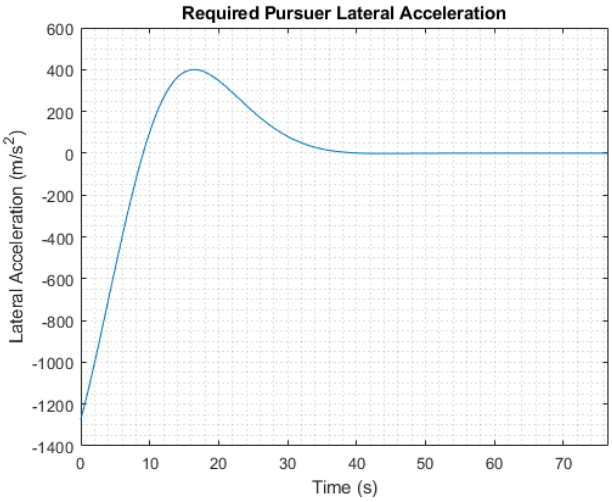

Fig. 14. Required Pursuer Lateral Acceleration, Pure Pursuit Guidance

The maximum acceleration magnitude required of the pursuer is found to be approximately 1273 $\frac{m}{s^2}$, this would be equivalent to an approximately 130g turn for the pursuer. Of note is that no limitations were placed on the maneuvering

capacity of the pursuer for this simulation, in a realistic scenario it would be exceedingly difficult for any actual vehicle to perform this turn if not flatly impossible. The lateral acceleration does go to zero at approximately 30 seconds when the tail chase is achieved, and no further control is required for the pursuer to remain in the tail chase. If the target were to maneuver this would change and the pursuer would need to maneuver to try to drive the pursuer velocity vector along the target LOS for far longer, requiring yet more maneuvering capacity from the pursuer. Maneuvering targets, however, are outside of the scope of this report and project and could be investigated at a future point in time.

Overall, planar pure pursuit guidance when under ideal conditions can give an intercept of a hypersonic target vehicle using a faster hypersonic pursuer. The performance of this guidance when compared to proportional navigation is notably inferior and as a result pure pursuit is a poor choice for the scenario under consideration. Indeed, pure pursuit is rarely used in a modern setting for interception. Proportional navigation is the more common method between the two, however pure pursuit does still see use in contexts such as stationary targets or for the navigation of autonomous vehicles (Shneydor).

The following section will present the motion camouflage pursuit law and its implementation for the case of hypersonic vehicle interception.

IV. Motion Camouflage

Motion camouflage (MC) is a pursuit method widely seen in nature. In the case of motion camouflage, the LOS is stabilized in the Inertial reference frame by the pursuer. For this pursuit method, the relative position and velocity of the target must be known (Shishika and Paley). To overcome this restriction of having to have knowledge of the target's steering, the control gain for the MC control law, μ, can be chosen to be positive and sufficiently large using high gain feedback. The pursuit law for MC can be written in a similar form to that of PPN. This form of the pursuit law is given by (Justh and Krishnaprasad):

$$u^{MC} = N\frac{|\vec{r}|}{r_0}\dot{\theta} \tag{31}$$

Where

$$N = \mu r_0 \tag{32}$$

The pursuit law represented by Equation 31 is proportional to the LOS angular rate and takes a similar form to the pursuit law used in PPN, as displayed by Equation 16. It should be noted that the relative position will now be described as the vector representing the position difference pursuer and the target ($\vec{r}_{P/T}$ or $\vec{r}$ for the sake of brevity). Due to how the steering is applied, a new coordinate system and reference frame(s) must be introduced as the setup used for proportional navigation is no longer convenient. The new coordinate system used will be the Normal - Tangent coordinate system. There are three reference frames, the inertial frame (similar to the original setup), and two body frames with their respective origins at the pursuer and the target. This setup can be seen in the figure below.

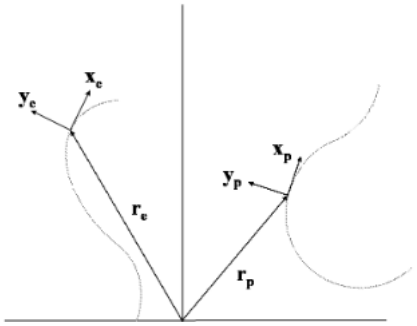

Fig. 15. Motion Camouflage Kinematic Model (Justh and Krishnaprasad)

The motion of both the target and pursuer can be described using the following equations known as the Frenet frame equations, where v is the in-plane speed (Mischiati and Krishnaprasad).

$$\dot{r}_i = v_i x_i \tag{33}$$

$$\dot{x}_i = v_i u_i y_i \tag{34}$$

$$\dot{y}_i = -v_i u_i x_i \tag{35}$$

In order to implement the pursuit law represented by Equation 31, an expression for the LOS angular rate must be introduced. The necessary expression is given below (Justh and Krishnaprasad). The $\perp$ operation represents a vector being rotated counter-clockwise in the plane by an angle of 90 degrees.

$$\dot{\theta} = -\frac{1}{|\vec{r}|}\left(\frac{\vec{r}}{|\vec{r}|}\cdot\dot{\vec{r}}^{\perp}\right) \tag{36}$$

It can be stated that the motion camouflage pursuit strategy holds when the metric for motion camouflage is equal to negative 1. This is because as the distance between the target and pursuer decreases, the LOS stabilizes as the metric approaches -1. The expression for this metric is given below (Shishika and Paley)

$$\Gamma = \frac{\vec{r}}{|\vec{r}|}\cdot\frac{\dot{\vec{r}}}{|\dot{\vec{r}}|} \tag{37}$$

Equation 31 can be re-written in a more general form given below. Interception is guaranteed using this pursuit law (and for Equation 31) for the conditions $\Gamma \neq 1$, $r_o > 0$, and the pursuer moves faster than the target along the bounded/continuous trajectories (Mischiati and Krishnaprasad).

$$u^{MC} = -\mu\left(\frac{\vec{r}}{|\vec{r}|}\cdot\dot{\vec{r}}^{\perp}\right) \tag{38}$$

A particularly interesting type of motion camouflage is known as Mutual Motion Camouflage. In this phenomenon

the two point masses are in mutual pursuit of one another, where both the target and pursuer are using the MC feedback law displayed in Equation 38. The closed loop dynamics for Mutual Motion Camouflage (MMC) are represented by a second order ordinary matrix differential equation. The dynamics are given below, and the full derivation can be seen in Mischiati and Krishnaprasad.

$$\ddot{\vec{r}} = -\mu[(\frac{\vec{r}}{|\vec{r}|}\cdot\dot{\vec{r}})\dot{\vec{r}} - |\dot{\vec{r}}|^2\frac{\vec{r}}{|\vec{r}|}] \tag{39}$$

A simulation was performed using these closed loop dynamics. A control gain of $\mu = 10$ was chosen, with an initial distance between the two masses of $r_0 = 1.5$ km with zero initial relative velocity (both masses are moving at the same speed initially). The peak relative velocity achieved is 1503 m/s. If this scenario is assumed to occur at an altitude of 15 km, this corresponds to a speed of Mach 5. The simulation results showing the magnitudes of the relative position and velocity are displayed below. From the results, we can see the relative distance goes to zero in about 6 seconds, along with the relative velocity. Therefore, it can be stated that the Motion Camouflage pursuit law was successfully implemented to achieve interception.

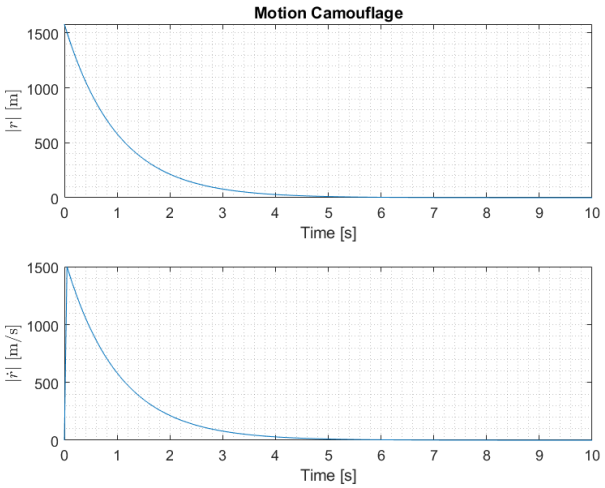

Fig. 16. Mutual Motion Camouflage Simulation

Conclusions

The three pursuit laws introduced in this paper, those being proportional navigation, simple pursuit, and motion camouflage, were all analyzed and implemented in simulation for the case of a non-maneuvering hypersonic target vehicle interception. The relative performance of the three approaches for the scenario was also considered, and there are some clear conclusions that can be drawn on that front.

Ideal proportional navigation was relatively simple to implement and notably effective for the given scenario, with the intercepts found to be realistic in implementation with regards to maximum accelerations and according stresses on the pursuing vehicle. For IPN, closed form solutions are attainable for key parameters such as the relative velocity and the total interception time. For implementation, a numerical integrator was used to generate the time history of all key states. Augmenting IPN to account for a maneuvering target required only the addition of two terms to the equations of motion governing the dynamics. Another form of proportional navigation, known as pure proportional navigation was also introduced. For PPN, the command acceleration is perpendicular to the velocity vector, unlike IPN where it is applied normal to the relative velocity vector. The pursuit law governing IPN was also introduced. Through implementation, it was found that proportional navigation was an effective pursuit law for the use of hypersonic interception.

Pure pursuit guidance, while simple to implement due to the assumptions made in the model and other simplifications of the engagement geometry and relevant physics, was found to be lacking for the scenario under consideration. The nature of the pursuit law resulted in the simulations turning into tail chases where the pursuer must be faster than the target to force an intercept, itself a limitation, as well as demanding large sums of energy from the pursuer to close with the target with a relatively low relative velocity. Additionally, since the pursuit law requires the velocity vector of the pursuer to lie directly along the LOS high lateral accelerations were demanded of the pursuer. This was especially exacerbated by the velocities involved in the problem, with a peak required lateral acceleration of over 1200 $\frac{m}{s^2}$. The successful interception of the target vehicle may then have only occurred due to no limitations on the maneuvering capacity of the pursuer having been applied for the simulation. As a result, pure pursuit is not a particularly effective approach for the interception of a hypersonic vehicle.

Motion camouflage is a newer pursuit method, and is one that is commonly found in nature. Motion camouflage itself depends directly on the stabilisation of the line of sight, and this stabilisation is quantified using the line of sight metric. Its application for the purpose of missile guidance is fairly under developed, and only a few papers have been written on this topic. Despite this, an attempt at implementation was made using a specific form of motion camouflage known as Mutual Motion Camouflage (MMC). Closed form solutions exist for MMC, and thus was implemented. The results showed a successful implementation, and provide evidence that Motion Camouflage may be a feasible pursuit law option for hypersonic vehicle interception, and missile guidance in general.

Future Work

Potential areas of future work for this topic include the analysis of further pursuit laws or variations of those presented in this paper. An example of this would be deviated pure pursuit for a non-maneuvering target, such as lead pursuit, or the implementation of pure proportional navigation (PPN).

Another area of future research could be the investigation of the case of a maneuvering hypersonic target for all of the considered pursuit laws. This would greatly increase the complexity of the pursuit and interception scenario and could potentially be the topic of its own project or report.

This was briefly introduced in the case of ideal proportional navigation, but further research and implementation using true or generalized proportional navigation may also be worthwhile. The extension of these pursuit laws to the three-dimensional case also warrants future research and development.

Lastly, it should be noted that the topic of the research paper that is presented here underwent a significant pivot relatively late in the semester and as such the scope for this report was limited to guarantee that results were attained for the three guidance laws that were selected.

References

P.-J. Yuan and J.-S. Chern, "Ideal Proportional Navigation," AIAA JOURNAL OF GUIDANCE, CONTROL, AND DYNAMICS, Sep-1992

D. Shishika and D. Paley, "MOSQUITO-INSPIRED SWARMING AND PURSUIT FOR AUTONOMOUS ROTORCRAFT," 2017.

K. Li, T. Zhang, and L. Chen, "Ideal Proportional Navigation for Exoatmospheric Interception," Chinese Journal of Aeronautics, vol. 26, no. 4, pp. 976–985, 2013.

N.A. Shneydor, Missile Guidance and Pursuit: Kinematics, Dynamics and Control, Cambridge, UK: Woodhead Publishing Ltd., 1998.

E. W. Justh and P. S. Krishnaprasad, "Steering laws for motion camouflage," Proceedings of the Royal Society A: Mathematical, Physical and Engineering Sciences, vol. 462, no. 2076, pp. 3629–3643, 2006.

M. Mischiati and P. S. Krishnaprasad, "Mutual motion camouflage in 3D*," IFAC Proceedings Volumes, vol. 44, no. 1, pp. 4483–4488, 2011.